High selectivity of TiC-CDC for CO_2/N_2 separation

Ana Silvestre-Albero[1], Soledad Rico-Francés[1], Francisco Rodríguez-Reinoso[1], Andreas M. Kern[2], Michael Klumpp[2], Bastian J.M. Etzold[2], Joaquin Silvestre-Albero[1,]*

[1]*Laboratorio de Materiales Avanzados, Departamento de Química Inorgánica-Instituto Universitario de Materiales, Universidad de Alicante E-03080 Alicante (Spain)*

[2]*Friedrich-Alexander Universität Erlangen-Nürnberg, Lehrstuhl für Chemische Reaktionstechnik, Egerlandstr. 3, 91058 Erlangen (Germany)*

Abstract

A series of carbide-derived carbons (CDC) have been prepared starting from TiC and using different chlorine treatment temperatures (500ºC-1200ºC). Contrary to N_2 adsorption measurements at -196ºC, CO_2 adsorption measurements at room temperature and high pressure (up to 1 MPa) together with immersion calorimetry measurements into dichloromethane suggest that the synthesized CDC exhibit a similar porous structure, in terms of narrow pore volume, independently of the temperature of the reactive extraction treatment used (samples synthesized below 1000ºC). Apparently, these carbide-derived carbons exhibit narrow constrictions were CO_2 adsorption under standard conditions (0ºC and atmospheric pressure) is kinetically restricted. The same accounts for a slightly larger molecule as N_2 at a lower adsorption temperature (-196ºC), i.e. textural parameters obtained from N_2 adsorption measurements on CDC

must be underestimated. Furthermore, here we show experimentally that nitrogen exhibits an unusual behavior, poor affinity, on these carbide-derived carbons. CH_4 with a slightly larger diameter (0.39 nm) is able to partially access the inner porous structure whereas N_2, with a slightly smaller diameter (0.36 nm), does not. Consequently, these CDC can be envisaged as excellent sorbent for selective CO_2 capture in flue-gas streams.

***Corresponding author**

Tel.: +34 96 590 9350/ Fax: +34 96 590 3454

Email: joaquin.silvestre@ua.es (J. Silvestre-Albero)

1. Introduction

CO_2 capture by gas adsorption using inorganic porous solids, e.g. zeolites, activated carbons, carbon molecular sieves, MOFs, and so on, is becoming a challenging task in terms of efficiency and economical issues for carbon capture & storage technologies (CCS) [1-4]. Both the porous structure and the surface chemistry of these materials are critical parameters to be designed in order to achieve an optimum adsorption capacity. Besides achieving a high adsorption capacity, newly designed adsorbents must be able to separate CO_2 from molecules of similar molecular dimensions as CH_4 or N_2 typically present in industrial effluents, i.e. molecular sieving properties are furthermore required. Among the different sorbents, carbon materials exhibit certain advantages for the aforementioned requirements such as high surface area, large micropore volume and, more importantly, the possibility to finely tailor the porous structure and surface chemistry accordingly by pre- and post-synthesis methods [5].

Carbide-derived carbons (CDC), prepared by the reactive extraction of metals from metal carbides with chlorine, are a relatively novel kind of porous carbons with tuneable pore structure, which attracted particular interest in the last few years e.g. in the fields of electrochemistry, gas storage and catalysis [6-14]. The pore size in these materials is highly influenced by the carbide precursor and reactive extraction temperature. Higher temperatures during synthesis may allow restructuring of the carbon to a higher degree of graphitization and larger pores are formed [6,15,16]. At lower synthesis temperatures carbon molecular sieves can result, which could be of interest for the application of gas separation, e.g. CO_2 separation in flue-gas streams.

The behavior of these carbon materials in gas separation (e.g. CO_2/N_2) would be highly defined by their porous network, i.e. a profound knowledge of the microporous structure

is mandatory. A variety of methods can be used to investigate the molecular sieve characteristics of carbons. Mainly used are equilibrium isotherms for N_2, CO_2 or Ar sorption to obtain with a variety of methods and models (e.g. condensation models like BJH or molecular simulation models like QSDFT) pore volume and pore size distributions. The pore structure can be further analyzed by small-angle scattering techniques like X-ray scattering (SAXS) or neutron scattering (SANS), which allows also probing closed pores. For titanium carbide-derived carbon (TiC-CDC), which is subject of this study, sorption isotherm analysis [16-22] and scattering [16,23-25] results are discussed in literature, showing that TiC-CDC synthesized below 900 °C shows pore sizes in the range of carbon molecular sieves. Equilibrium CO_2 adsorption isotherms demonstrated that with TiC-CDC high CO_2 uptakes can be realized [26]. For characterizing molecular sieves for the application in gas separation, two additional characterization methods are of major interest as they probe directly the accessibility of the pore volume for molecules. This is i) immersion calorimetry with different sized probe molecules (equilibrium measurements) [27] and ii) adsorption uptakes measured in the kinetic regime despite the equilibrium regime, which allow studying additional kinetic effects, which can be used for gas separation. Both methods were employed within this work and combined with high resolution N_2 and low and high pressure CO_2 isotherms, including adsorption and desorption branches, to discuss accessibility of the microporosity and achievable CO_2/N_2 and CH_4/N_2 selectivity when using carbide-derived carbons as sorbents.

2. Experimental Section

2.1. Synthesis of carbide-derived carbons

Carbide-derived carbons were synthesized starting from commercial TiC powder (99.5 % purity, approximately 3.5 µm in diameter, Alfa Aesar GmbH & Co KG). The reactive extraction treatment with chlorine is described in detail elsewhere [28,29]. Briefly, the powders were held by a graphite crucible, which is placed in the isothermal zone of a horizontal tubular reactor (Al_2O_3, d = 3.2 cm, l = 1.3 m), lined by thin graphite foil. The reactor was evacuated and then heated to the desired extraction temperature (500, 700, 900, 1200 °C) under constant helium flow. At reaction temperature the reaction was started by dosing chlorine (1 mol m^{-3} in helium, 0.25 m s^{-1}). After 4 hours the extraction was stopped by purging with helium for 30 minutes. Afterwards, the samples were flushed for 30 minutes with a hydrogen/helium mixture (20 vol.-% H_2) at the extraction temperature (except TiC-CDC chlorinated at 500 °C, which was H_2 treated at 600°C) and cooled down in Helium atmosphere. Materials are referred to according to their synthesis temperature TiC-CDC-500, TiC-CDC-700, TiC-CDC-900 and TiC-CDC-1200.

2.2. Sample characterization

Gas adsorption measurements (N_2 at -196ºC and CO_2 at 0ºC) at atmospheric pressure were performed in a home-made fully automated equipment designed and constructed by the Advanced Materials group (LMA), now commercialized as N_2Gsorb-6 (Gas to Materials Technologies; www.g2mtech.com). High-pressure analysis (in this work up to 1 MPa) were performed in a home-made fully automated equipment designed and constructed by the Advanced Materials group (LMA), now commercialized as iSorbHP

by Quantachrome Instruments. Before any experiment, samples were degassed (10^{-8} MPa) at 150ºC for 4h. Textural parameters (BET "apparent" surface area and micropore volume, V_{micro}) were estimated from the nitrogen adsorption data after application of the BET and the Dubinin-Radushkevich equations, respectively. The volume of mesopores (V_{meso}) was estimated by subtracting the micropore volume (V_{micro}) to the total pore volume (V_t) measured at $p/p_0 \approx 0.95$.

Kinetic measurements were performed at 25ºC in a glass manometric equipment using pure gas components (CO_2, N_2 and CH_4). Prior to the adsorption experiment, the sample was degassed under vacuum (10^{-8} MPa) at 150ºC for 4h.

Immersion calorimetry measurements into liquids of different molecular dimensions were performed in a Tian-Calved C80D calorimeter at 30ºC. A complete description of the experimental equipment can be found elsewhere [27]. Briefly, before the immersion calorimetric measurement the sample was degassed at 150ºC for 4h in a glass bulb connected to a vacuum equipment. After the degassing step, the sample is sealed in vacuum and the glass bulb is transferred to the calorimetric chamber together with the liquid probe. After thermal equilibrium has been reached, the sample tip is broken and the sample is allowed to interact with the immersion liquid. The heat evolved during this process ($-\Delta H_{imm}$) is recorded with time. The surface area accessible to dichloromethane (S_{DCM}) was estimated for each sample from the corresponding heat of immersion after calibration using a non-porous reference carbon black (V3G).

3. Results and Discussion

3.1. Textural characterization

Figure 1 shows the nitrogen adsorption/desorption isotherms for the different carbide-derived carbons prepared using different temperatures for the chlorine treatment. As it can be observed, the CDC sample prepared at the lowest temperature (500ºC) exhibits a type I isotherm according to the IUPAC classification, characteristic of a pure microporous sample [28]. The presence of a narrow knee in the nitrogen isotherm at low relative pressures anticipates the presence of a narrow pore size distribution (PSD). An increase in the chlorine treatment temperature to 700ºC produces an increase in the amount of nitrogen adsorbed, this effect being even larger in the sample chemically treated at 900ºC. Additionally, sample TiC-CDC-900 exhibits a widening in the low-pressure knee of the nitrogen isotherm, thus suggesting the formation of wider micropores at these high temperatures. A further increase in the chlorine treatment temperature above 1000ºC becomes detrimental for the textural properties, i.e. there is a certain collapse of the porous structure, together with the development of mesoporosity (see Table 1). It is well-known that temperatures above 1000ºC gives rise to the graphitization of the carbon structure which is accompanied by the development of mesoporosity and a partial collapse of the microporous network. The sudden changes in the porosity can be clearly reflected by the modification of the nitrogen isotherm (type II and IV) together with the presence of a hysteresis loop at high-relative pressures.

Table 1 shows a compilation of the main textural properties obtained from the nitrogen adsorption data at -196ºC after application of the BET and the Dubinin-Radushkevich equations. In accordance with previous observations, an increase in the chlorine treatment temperature gives rise to a development of porosity, i.e. an increase in the

"apparent" surface area and total micropore volume up to 900ºC, the situation being modified thereafter. In any case, it is important to highlight that nitrogen adsorption measurements clearly reflect important changes in the porous structure of these carbon materials with the extraction temperature.

A similar conclusion can be obtained after application of mathematical models based on the density-functional theory (QSDFT) to the N_2 adsorption data at -196ºC. The pore size distribution (PSD) obtained using a slit/cylindr-shape pore model anticipates: i) the presence of narrow micropores (pores around 0.6-0.8 nm) on these CDC, ii) the presence of important changes in the microporous structure (pore size and volume) after an increase in the chlorine treatment temperature and iii) the development of wide micropores above 700ºC and mesopores above 1000ºC. The specific surface area (SSA) estimated using the QSDFT model (see Table 1) follows the same tendency achieved with the BET equation, i.e. there is an increase in the accessible surface area up to sample TiC-CDC-900, the SSA decreasing thereafter.

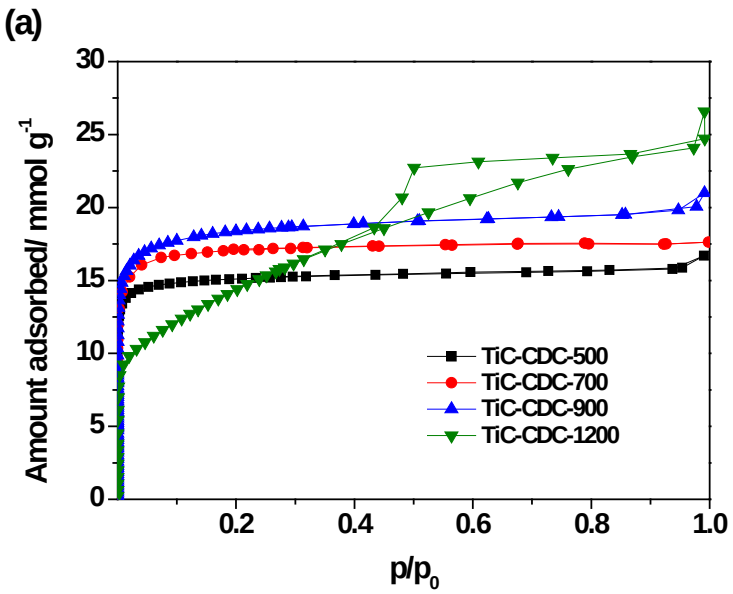

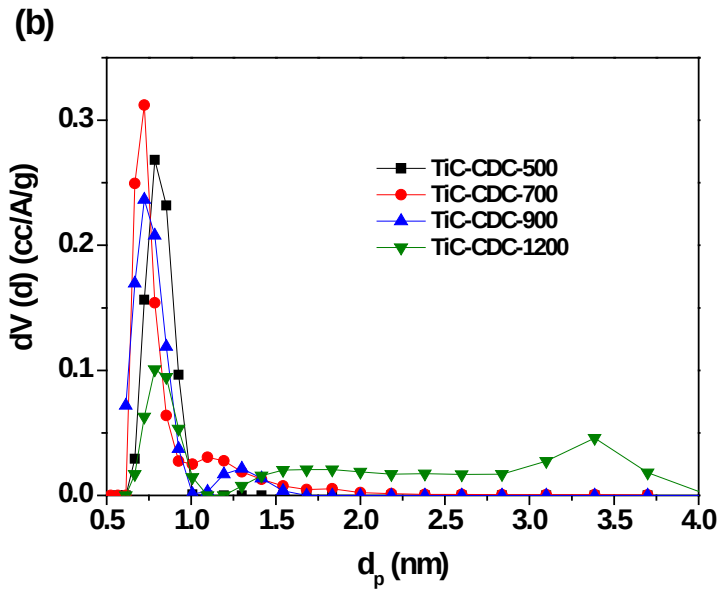

Figure 1. (a) N_2 adsorption/desorption isotherms at -196ºC for the different TiC-CDC samples; (b) pore size distribution after application of the QSDFT method to the N_2 adsorption data at -196ºC (slit/cylindr-shape pore morphology; equilibrium model).

Table 1. Textural properties for the different carbide-derived carbons obtained from the nitrogen adsorption data at -196ºC and immersion calorimetry into dichloromethane.

Sample	S_{BET} / $m^2\ g^{-1}$	V_{micro} / $cm^3\ g^{-1}$	V_{meso} / $cm^3\ g^{-1}$	V_t / $cm^3\ g^{-1}$	S_{DCM} / $m^2\ g^{-1}$	S_{QSDFT} / $m^2\ g^{-1}$
TiC-CDC-500	1340	0.52	0.03	0.55	1461	1250
TiC-CDC-700	1490	0.58	0.04	0.62	1439	1434
TiC-CDC-900	1580	0.62	0.11	0.73	1508	1497
TiC-CDC-1200	1165	0.39	0.44	0.83	827	984

A powerful technique for the characterization of the textural properties of a porous solid is immersion calorimetry. In the absence of specific interactions at the liquid-solid interface, the heat of interaction of a certain liquid with the porous surface can be used to estimate the accessible surface area and, by selecting molecules of

different molecular dimensions, the pore size distribution [27]. Figure 2 shows the heat of immersion for three different molecules with a different kinetic diameter, i.e. dichloromethane (0.33 nm), 2,2-dimethylbutane (0.56 nm) and α-pynene (0.7 nm). Interestingly, a small molecule such as dichloromethane gives an enthalpy of immersion around 160-170 J g^{-1} for all the samples except CDC-1200 sample. As described above, in the absence of specific interactions at the solid-liquid interface, the heat of immersion can be used to estimate the surface area available for a certain molecule after the appropriate calibration using a reference non-porous solid with similar characteristics. In the case of carbide-derived carbons, the surface area accessible to dichloromethane after calibration using a non-porous carbon black as a reference (V3G) provides an estimated value around 1450-1500 m^2 g^{-1} for all the CDC except the sample synthesized at high temperature. Interestingly, these values are very close to the BET surface area estimated from the nitrogen adsorption data at -196ºC, at least for samples 700ºC and 900ºC, thus reflecting the validity of immersion calorimetry to estimate the textural properties of carbon materials. At this point it is interesting to highlight the absence of clear differences between the different CDC samples, as estimated from dichloromethane immersion calorimetry, independently of the chlorine treatment temperature used (excluding sample CDC-1200). This observation is somehow in contradiction with nitrogen adsorption measurements where a large improvement in the development of the microporosity was estimated after an increase in the reactive extraction temperature from 500ºC to 900ºC.

Immersion calorimetry using larger molecules produce a decrease in the heat of interaction, hence in the accessible specific surface area, this effect being more drastic for sample TiC-CDC-500 where α-pynene (kinetic diameter 0.7 nm) exhibits a limited

accessibility, i.e. the heat of immersion being quite small. The observed results anticipate that sample TiC-CDC-500 is a carbon molecular sieve, i.e. molecules above 0.7 nm will not be able to access completely the inner porosity, this molecular sieving behavior disappearing above 500ºC.

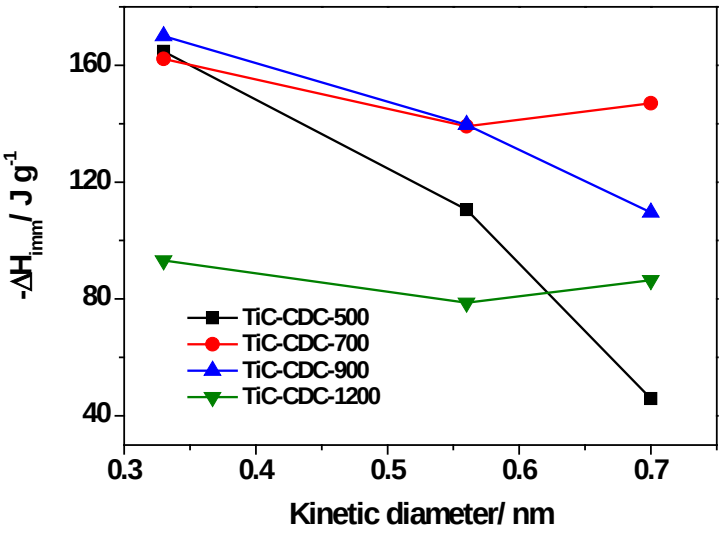

Figure 2. Heat of immersion (J g^{-1}) for molecules of different kinetic diameter for the different CDC samples. Immersion liquids are dichloromethane (0.33 nm), 2,2-dimethylbutane (0.56 nm) and α-pynene (0.7 nm).

3.2. CO_2 adsorption analysis at atmospheric and high pressure

Adsorption analysis at atmospheric pressure using a slightly smaller molecule compared to N_2 as CO_2 (0.36 nm vs. 0.33 nm) and a higher adsorption temperature (0ºC vs. -196ºC) has been proposed by some of us for the characterization of the narrow microporosity in porous solids (pores below 0.7 nm) [29,30]. Furthermore, CO_2 adsorption can be used to evaluate the presence of narrow constrictions usually

inaccessible to N_2 at cryogenic temperatures [31]. Figure 3a shows the CO_2 adsorption/desorption isotherms for the different carbide-derived carbons samples at 0ºC and atmospheric pressure. As it can be observed, even when using an equilibration time of 120s all isotherms exhibit a slight delay between the adsorption and the desorption branch, i.e. the desorption branch is not able to match perfectly the adsorption branch. This behavior clearly reflects the lack of real equilibrium in the adsorption branch even though a high equilibration time has been used during the performance of the isotherms, i.e. these carbide-derived carbons must contain narrow constrictions where CO_2 exhibit problems of accessibility [32]. Taking into account previous analysis described in the literature, one can suspect that these narrow constrictions would be inaccessible to nitrogen at -196ºC [31]. As expected from the results described above, the adsorption capacity for CO_2 increases with the chlorine treatment temperature up to 700ºC, the amount adsorbed decreasing thereafter. The decline in the adsorption capacity for sample TiC-CDC-900 would confirm the importance of narrow micropores in CO_2 adsorption, in close agreement with the literature [26]. Furthermore, the delay between the adsorption and the desorption branches diminished with the increase in the extraction temperature (900 °C, 1200 °C), thus reflecting either a smaller concentration of narrow constrictions or a partial narrowing of the already existing microporosity, i.e. high synthesis temperatures favor the shrinkage of the microporous structure in such a way that narrow constrictions are closed or vanish on these samples chlorinated at high temperatures. During the reactive extraction of the carbide unsaturated carbon dangling bonds occur, when braking up the carbon metal bond. At higher extraction temperature the carbon could be more mobile before recombining, which is to a certain extend proven by the higher degree of graphitization for higher extraction temperatures. This higher mobility during the

carbide-derived carbon network formation is supposed to be responsible for the aforementioned described effects.

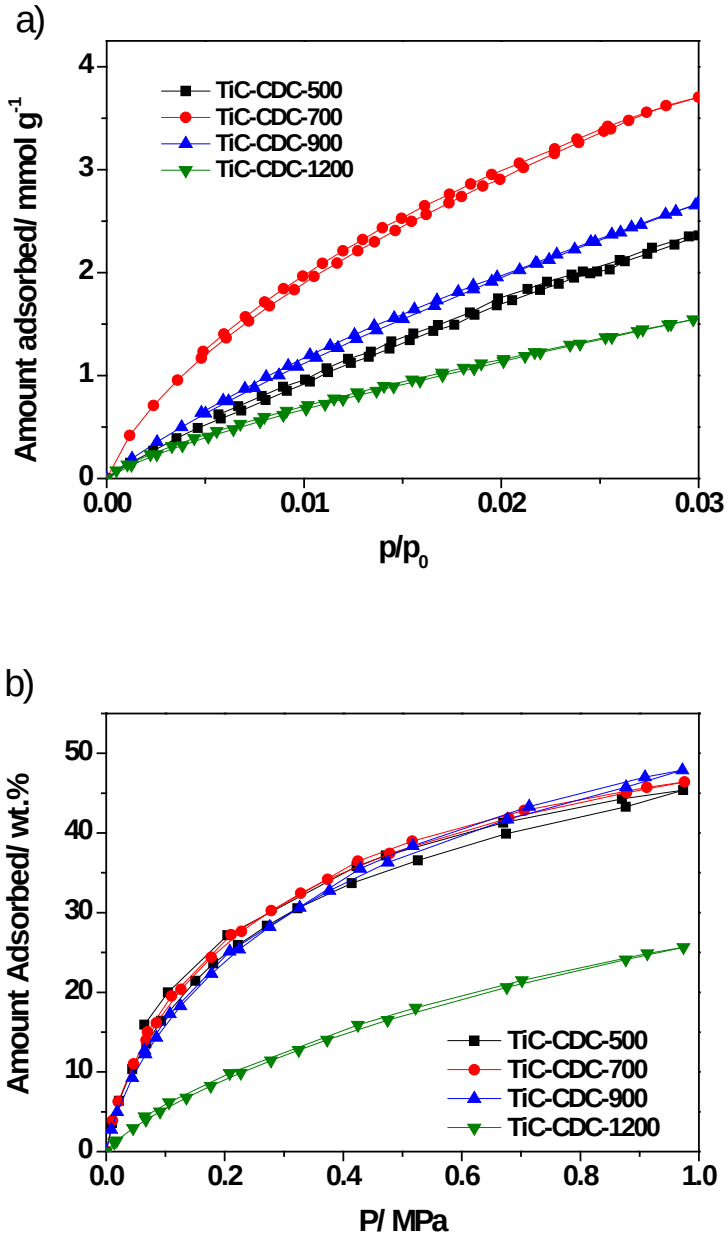

Figure 3. CO_2 sorption isotherms up to (a) atmospheric pressure and 0ºC and (b) high pressure (1 MPa) and 25ºC, for the different carbide-derived carbons (equilibration time 120s).

Recent analysis described in the literature has shown that carbon materials are excellent candidates for CO_2 capture both at atmospheric and high pressure [1,2,26,33]. Taking into account that an optimum carbon for CO_2 capture requires the presence of a well-developed narrow microporosity (pores below 0.8 nm for atmospheric pressure studies), carbide-derived carbons can be anticipated as excellent candidates in terms of adsorption capacity and selectivity towards molecules of similar molecular dimensions. In this sense, Figure 3b shows the behavior of the different carbide-derived samples in the adsorption of CO_2 up to high pressure (1 MPa) and 25ºC. Surprisingly, all samples except CDC-1200 perform equal in terms of adsorption capacity for CO_2 at high pressure (see Table 2) with a maximum adsorption capacity of 480 mg g^{-1} at 1.0 MPa. Previous studies described in the literature using similar materials have shown that CO_2 adsorption capacity correlates with the total volume of specific pores depending on the final pressure achieved [26]. Whereas narrow micropores (<0.5 nm) are responsible for the adsorption capacity at 0.01 MPa, larger micropores (<0.8 nm) defines the adsorption capacity at atmospheric pressure. Taking into account these premises and the final pressure achieved in Figure 3b (1.0 MPa), which corresponds to a $p/p_0 \sim 0.16$, these results suggest that samples TiC-CDC-500, TiC-CDC-700 and TiC-CDC-900 must exhibit a similar porous structure in terms of total micropore volume, i.e., at $p/p_0 \sim 0.16$ mainly all micropores must be already filled. The similarity in the adsorption isotherms for these three samples when using CO_2 is in close agreement with calorimetric measurements using a molecule with a similar dimension as dichloromethane (0.33 nm). Apparently, these carbide-derived carbons exhibit inner cavities accessible via narrow constrictions which can only be surpassed either using “higher” adsorption temperatures (25ºC) and/or a higher pressures (1 MPa), compared to the traditional measurement at 0ºC and atmospheric pressure.

Table 2. Total amount of CO_2 adsorbed at atmospheric pressure and high pressure$^{\delta}$ (1.0 MPa) in the different carbide-derived carbons under equilibrium conditions. CO_2/CH_4 and CO_2/N_2 selectivity derived in a kinetic regime at 25ºC and after t= 2min.

Sample	Amount adsorbed/ mg g^{-1}	Amount adsorbed$^{\delta}$/ mg g^{-1}	$S(CO_2/CH_4)$	$S(CO_2/N_2)$
TiC-CDC-500	97	452	2.6	∞
TiC-CDC-700	161	466	2.8	19
TiC-CDC-900	120	480	8.3	∞
TiC-CDC-1200	49	256	∞	∞

In summary, CO_2 adsorption measurements in combination with immersion calorimetry suggest that carbide-derived carbons prepared from TiC exhibit a similar porous structure independently of the chlorine treatment temperature used, at least for temperatures below 1000ºC. Calorimetric measurements using molecules of different dimensions suggest that the chlorine extraction temperature mainly affects the pore size opening, i.e. the pore entrance is widened after an increase in the extraction temperature. The presence of kinetic restrictions for CO_2 adsorption at 0ºC and atmospheric pressure can be clearly extrapolated to a larger molecule as N_2 at a lower adsorption temperature (-196ºC), i.e. textural characteristics obtained from the nitrogen adsorption isotherms (e.g. BET surface area) must be underestimated, in agreement with previous studies on similar materials using SANS [34,35].

3.3. Kinetic analysis of single gas adsorption (N_2, CO_2 and CH_4)

The adsorption kinetics of nitrogen (0.36 nm), carbon dioxide (0.33 nm) and methane (0.39 nm) were analyzed at 25ºC in the different carbide-derived carbons using an initial gas pressure of 0.07 MPa. Figure 4 shows the adsorption kinetics for the different carbide-derived carbons using single pure gases. In general, adsorption kinetics is fast in all the samples for the different probe molecules considered (95% of the total adsorption capacity is achieved within few seconds). As expected, carbon dioxide with the lowest kinetic diameter (0.33 nm) is the most adsorbed gas for all samples. In accordance with previous adsorption measurements the total amount of carbon dioxide adsorbed increases after an increase in the extraction temperature to 700ºC, the amount adsorbed drastically decreasing thereafter. Surprisingly, whereas nitrogen adsorption is mainly nil for all samples studied, a slightly larger molecule as methane (0.39 vs. 0.36 nm) is able to partially access the inner porous structure of the carbide-derived carbons. In any case, the total amount adsorbed of methane and nitrogen slightly increases for sample TiC-CDC-700, the amount adsorbed being mainly nil for the samples synthesized above this temperature. The larger adsorption of methane compared to nitrogen is completely opposite to the typical behavior observed in the literature for carbon molecular sieves, which is defined based on kinetic considerations [33]. The observed behavior on the carbide-derived carbon molecular sieves allows for a large CO_2/N_2 selectivity (within the accuracy of the equipment ∞) compared to conventional carbon molecular sieves, except sample CDC-700. Concerning the CO_2/CH_4 selectivity, it increases with the increase in the chlorine treatment temperature up to an infinite value for sample CDC-1200 although associated with a lower adsorption capacity (see Table 2).

In summary, adsorption kinetics anticipate that carbide-derived carbons are promising candidates for CO_2 separation from N_2 in flue gas streams at room temperature and atmospheric pressure with extremely high selectivity values, independently of the chlorine treatment temperature used. To our knowledge these are the best results reported in the literature, in terms of separation capacity, for CO_2/N_2 using carbon molecular sieves.

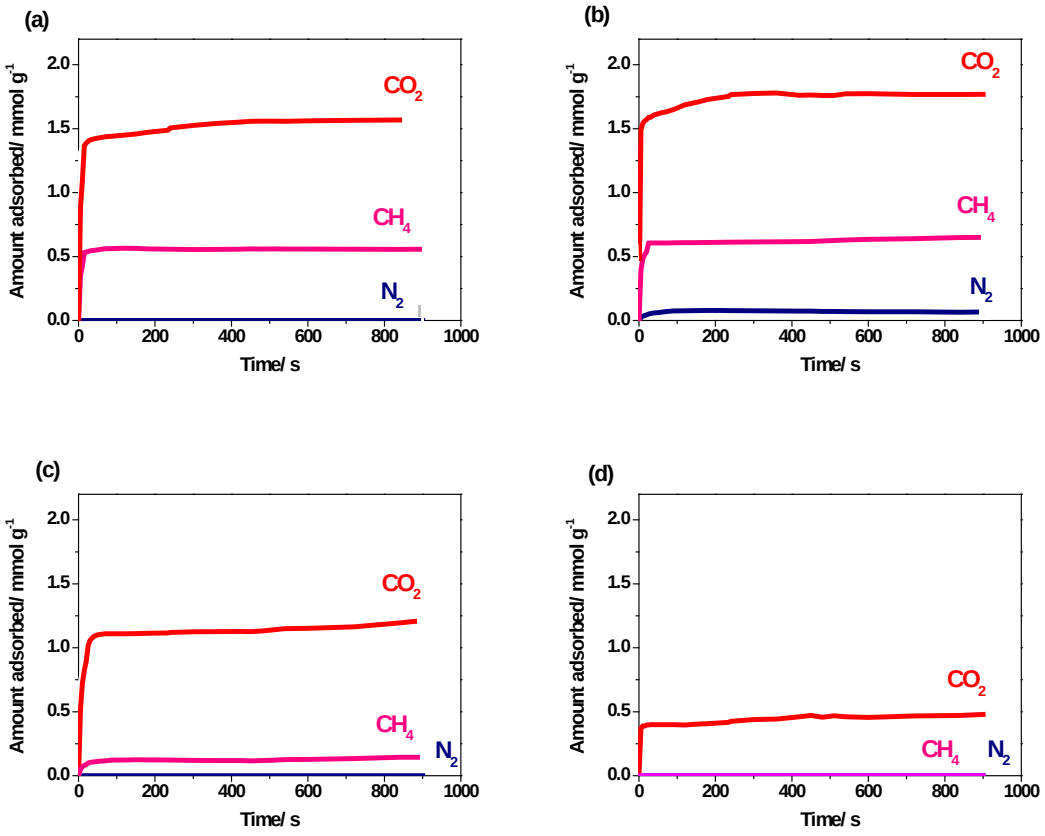

Figure 4. CO_2, CH_4 and N_2 adsorption kinetics for the different carbide-derived carbons, (a) TiC-CDC-500, (b) TiC-CDC-700, (c) TiC-CDC-900 and (d) TiC-CDC-1200, at 25ºC and 0.07 MPa initial pressure.

3.4. N_2, CO_2 and CH_4 comparative adsorption studies at atmospheric pressure

Finally, the adsorption capacity of the sample TiC-CDC-700 has been analyzed under equilibrium conditions and atmospheric pressure for CO_2, N_2 and CH_4 at 25ºC. It is noteworthy to mention that under these experimental conditions, CO_2 is in subcritical conditions whereas CH_4 and N_2 are in supercritical conditions. As it can be observed in Figure 5, equilibrium data confirm the observations described before for kinetic analysis, i.e. nitrogen accessibility to the inner porosity in carbide-derived carbons is partly inhibited. The prevalence of this behavior even under equilibrium conditions (120s equilibration time) clearly suggest that nitrogen accessibility is restricted not due to kinetic limitations but rather to other phenomena, i.e., the presence of an unexpected low affinity of CDC for N_2. At this point is again interestingly to highlight that a "larger" molecule as CH_4 is able to access the inner porosity whereas nitrogen does not. Consequently, the inaccessibility of nitrogen to the inner porous structure on these materials must be probably associated to specific interactions at the pore mouth with the nitrogen molecule, most probably associated with its quadrupole moment, which allow us to claim these CDC as excellent materials for the selective adsorption of CO_2 on nitrogen rich effluents, e.g. flue-gas streams from power plants. Although grand canonical Monte Carlo (GCMC) simulations anticipated a weak adsorption of N_2 on similar carbide-derived carbons [36], further analysis and/or theoretical calculations are required in order to fully understand the real nature of the inaccessibility or low affinity of nitrogen to the inner porous structure in carbide-derived carbon materials.

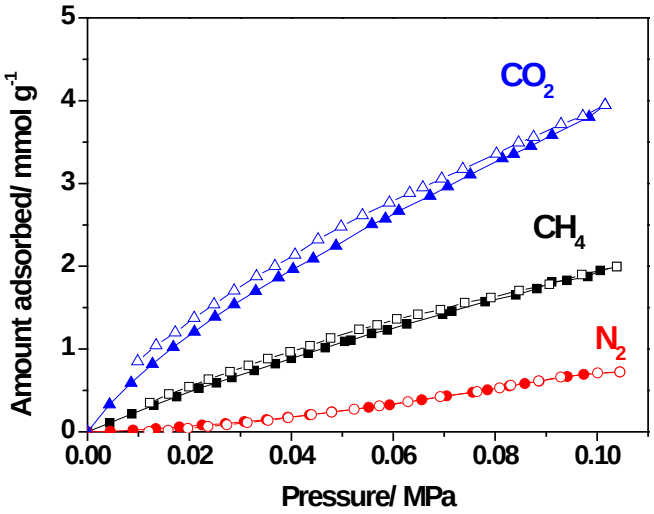

Figure 5. CO_2, CH_4 and N_2 sorption isotherms for sample TiC-CDC-700 at 25ºC.

A final prove about the presence of narrow constrictions in these CDCs comes from the comparison of the CO_2 adsorption isotherms for sample TiC-CDC-700 at atmospheric pressure and two different adsorption temperatures, i.e. 0ºC (Figure 3a) and 25ºC (Figure 5). Contrary to thermodynamic considerations, CO_2 uptake slightly increases with the adsorption temperature (3.93 mmol/g at 25ºC vs. 3.72 mmol/g at 0ºC). This observation clearly reflects an increase in the kinetics of adsorption into the narrow constrictions at 25ºC. Furthermore, the presence of a larger delay between the adsorption and desorption branches at 25ºC clearly reflects the difficulty to attain real equilibrium in these narrow constrictions, inaccessible to CO_2 at 0ºC, even at this "high" temperature.

Conclusions

A series of carbide-derived carbons have been successfully prepared starting from TiC and using a chlorine treatment at different temperatures. N_2 adsorption measurements suggest a real effect of the chlorine treatment temperature in the development of porosity, mainly microporosity, which is denied by CO_2 adsorption measurements at high pressure and/or high temperature and calorimetric analysis. These two analyses suggest that the porous structure of these CDCs is mainly unaffected in terms of pore volume after an increase in the temperature of the chlorine treatment (except samples treated above 1000ºC), i.e. the textural properties estimated from nitrogen adsorption must be underestimated. Furthermore, gas separation analysis shows that these CDCs are excellent materials for the complex CO_2 separation from N_2, i.e. nitrogen accessibility at room temperature and atmospheric pressure is inhibited compared to larger molecules (e.g. CH_4) probably due to specific interactions at the pore mouth.

Acknowledgement

Authors acknowledge financial support from the MICINN (project PLE2009-0052) and Generalitat Valenciana (PROMETEO/2009/002). AK, MK and BE gratefully acknowledge the funding of the German Research Council (DFG), which within the framework of its "Excellence Initiative" supports the Cluster of Excellence "Engineering of Advance Materials" (www.eam.uni-erlangen.de) at the University of Erlangen-Nuremberg.

References

[1] Silvestre-Albero J, Wahby A, Sepúlveda-Escribano A, Martínez-Escandell M, Kaneko K, Rodríguez-Reinoso F. Ultrahigh CO_2 adsorption capacity on carbon molecular sieves at room temperature. Chem. Commun. 2011; 47: 6840-42.

[2] Sevilla M, Fuertes AB. Sustainable porous carbons with a superior performance for CO_2 capture. Energy & Environ. Sci. 2011; 4: 1765-71.

[3] Yazaydin AÖ, Snurr RQ, Park T-H, Koh K, Liu J, LeVan MD, et al. Screening of metal-organic frameworks for carbon dioxide capture from flue gas using a combined experimental and modeling approach. J. Am. Chem. Soc. 2009; 131: 18198-99.

[4] D´Alessandro DM, Smit B, Long JR. Carbon dioxide capture: Prospects for new materials. Angew. Chem. Int. Ed. 2010; 49: 6058-82.

[5] Marsh H, Rodríguez-Reinoso F. Activated Carbon. Oxford: Elsevier; 2006.

[6] Presser V, Heon M, Gogotsi Y. Carbide-derived carbons-From porous networks to nanotubes and graphene. Adv. Funct. Mater. 2011; 21: 810-33.

[7] Gogotsi Y, Nikitin A, Ye H, Zhou W, Fischer JE, Yi B, et al. Nanoporous carbide-derived carbon with tunable pore size. Nature Materials 2003; 2: 591-94.

[8] Borchardt L, Oschatz M, Lohe M, Presser V, Gogotsi Y, Kaskel S. Ordered mesoporous carbide-derived carbons prepared by soft templating. Carbon 2012; 50: 3987-94.

[9] Krawiec P, Kockrick E, Borchardt L, Geiger D, Corma A, Kaskel S. Ordered mesoporous carbide derived carbons: Novel materials for catalysis and adsorption. J. Phys. Chem. C 2009; 113: 7755-61.

[10] Jänes A, Permann L, Arulepp A, Lust E. Electrochemical characteristics of nanoporous carbide-derived carbon materials in nonaqueous electrolyte solutions. Electrochem. Commun. 2004; 6: 313-8.

[11] Tallo I, Thomberg T, Kontturi K, Jänes A, Lust E. Nanostructured carbide-derived carbon synthesized by chlorination of tungsten carbide. Carbon 2011; 49: 4427-33.

[12] Glenk F, Knorr T, Schirmer M, Gütlein S, Etzold BJM. Synthesis of microporous carbon foams as catalyst supports. Chem. Eng. Techn. 2010; 33: 698-703.

[13] Knorr T, Heinl P, Schwerdtfeger J, Körner C, Singer RF, Etzold BJM. Process specific catalyst supports-Selective electron beam melted cellular metal structures coated with microporous carbon. Chem. Eng. J. 2012; 181-182: 725-33.

[14] Schmirler M, Glenk F, Etzold BJM. In-situ thermal activation of carbide-derived carbon. Carbon 2011; 49: 3679-86.

[15] Urbonaite S, Hälldahl L, Svensson G. Raman spectroscopy studies of carbide derived carbons. Carbon 2008; 46: 1942-47.

[16] Dash R, Chmiola J, Yushin G, Gogotsi Y, Laudisio G, Singer J, et al. Titanium carbide derived nanoporous carbon for energy-related applications. Carbon 2006; 44: 2489-97.

[17] Becker P, Glenk F, Kormann M, Popovska N, Etzold BJM. Chlorination of titanium carbide for the processing of nanoporous carbon: A kinetic study. Chem. Eng. J. 2010; 159: 236-41.

[18] Zetterström P, Urbonaite S, Lindberg F, Delaplane RG, Leis J, Svensson G. Reverse Monte Carlo studies of nanoporous carbon from TiC. J. Physics: Condensed Matter 2005; 17: 3509-24.

[19] Palmer JC, Llobet A, Yeon S-H, Fischer JE, Shi Y, Gogotsi Y, et al. Modeling the structural evolution of carbide-derived carbons using quenched molecular dynamics. Carbon 2010; 48: 1116-23.

[20] Kormann M, Gerhard H, Popovska N. Comparative study of carbide-derived carbons obtained from biomorphic TiC and SiC structures. Carbon 2009; 47: 242-50.

[21] Kormann M, Ghanem H, Gerhard H, Popovska N. Processing of carbide-derived carbon (CDC) using biomorphic porous titanium carbide ceramics. J. European Ceramic Soc. 2008; 28: 1297-303.

[22] Zhao Y, Wang W, Xiong D-B, Shao G, Xia W, Yu S, et al. Titanium carbide derived nanoporous carbon for supercapacitor applications. International Journal of Hydrogen Energy 2012; 37: 19395-00.

[23] Laudisio G, Dash R, Singer JP, Yushin G, Gogotsi Y, Fischer JE. Carbide-derived carbons: a comparative study of porosity based on small-angle scattering and adsorption isotherms. Langmuir 2006; 22: 8945-50.

[24] Yeon S-H, Osswald S, Gogotsi Y, Singer JP, Simmons JM, Fischer JE et al. Enhanced methane storage of chemically and physically activated carbide-derived carbon. J. Power Sources 2009; 191: 560-67.

[25] He L, Chathoth SM, Melnichenko YB, Presser V, McDonough J, Gogotsi Y. Small-angle neutron scattering characterization of the structure of nanoporous carbons for energy-related applications. Microp. Mesop. Mater. 2012; 149: 46-54.

[26] Presser V, McDonough J, Yeon S-H, Gogotsi Y. Effect of pore size on carbon dioxide sorption by carbide derived carbon. Energy & Environ. Sci. 2011; 4: 3059-66.

[27] Silvestre-Albero J, Gómez-de-Salazar C, Sepúlveda-Escribano A, Rodríguez-Reinoso F. Characterization of microporous solids by immersion calorimetry. Colloid Surface A: Phys. & Eng. Aspects 2001; 187-188: 151-65.

[28] Sing KSW, Everett DH, Haul RAW, Moscou L, Pierotti RA, Rouquerol J, et al. Reporting physisorption data for gas/solid systems. Pure Appl. Chem. 1985; 57: 603-19.

[29] Rodríguez-Reinoso F, Garrido J, Martín-Martínez JM, Molina-Sabio M, Torregrosa R. The combined use of different approaches in the characterization of microporous carbons. Carbon 1989; 27: 23-32.

[30] Garrido J, Linares-Solano A, Martín-Martínez JM, Molina-Sabio M, Rodríguez-Reinoso F, Torregrosa R. Use of N_2 vs. CO_2 in the characterization of activated carbons. Langmuir 1987; 3: 76-81.

[31] Rios RVRA, Silvestre-Albero J, Sepúlveda-Escribano A, Molina-Sabio M, Rodríguez-Reinoso F. Kinetic restrictions in the characterization of narrow microporosity in carbon materials. J. Phys. Chem. C 2007; 111: 3803-05.

[32] Silvestre-Albero A, Juárez-Galán JM, Silvestre-Albero J, Rodríguez-Reinoso F. Low-pressure hysteresis in adsorption: An artifact?. J. Phys. Chem. C 2012; 116; 16652-55.

[33] Wahby A, Ramos-Fernández JM, Martínez-Escandell M, Sepúlveda-Escribano A, Silvestre-Albero J, Rodríguez-Reinoso F. High-surface-area carbon molecular sieves for selective CO_2 adsorption. ChemSusChem 2010; 3: 974-81.

[34] Nguyen TX, Bhatia SK. Characterization of accessible and inaccessible pore in microporous carbons by a combination of adsorption and small angle neutron scattering. Carbon 2012; 50: 3045-54.

[35] He L, Chathoh SM, Melnichenko YB, Presser V, McDonough J, Gogotsi Y. Small-angle neutron scattering characterization of the structure of nanoporous carbons for energy-related applications. Microp. Mesop. Mater. 2012; 149: 46-54.

[36] Bhatia SK, Nguyen TX. Potential of silicon carbide-derived carbon for carbon capture. Ind. Eng. Chem. Res. 2011; 50: 10380-83.

List of captions

Figures

Figure 1. (a) N_2 adsorption/desorption isotherms at -196ºC for the different TiC-CDC samples; (b) pore size distribution after application of the QSDFT method to the N_2 adsorption data at -196ºC (slit/cylindr-shape pore morphology; equilibrium model).

Figure 2. Heat of immersion (J g^{-1}) for molecules of different kinetic diameter for the different CDC samples. Immersion liquids are dichloromethane (0.33 nm), 2,2-dimethylbutane (0.56 nm) and α-pynene (0.7 nm).

Figure 3. CO_2 sorption isotherms up to (a) atmospheric pressure and 0ºC and (b) high pressure (1 MPa) and 25ºC, for the different carbide-derived carbons (equilibration time 300s).

Figure 4. CO_2, CH_4 and N_2 adsorption kinetics for the different carbide-derived carbons, (a) TiC-CDC-500, (b) TiC-CDC-700, (c) TiC-CDC-900 and (d) TiC-CDC-1200, at 25ºC and 0.07 MPa initial pressure.

Figure 5. CO_2, CH_4 and N_2 sorption isotherms for sample TiC-CDC-700 at 25ºC.

Tables

Table 1. Textural properties for the different carbide-derived carbons obtained from the nitrogen adsorption data at -196ºC and immersion calorimetry into dichloromethane.

Table 2. Total amount of CO_2 adsorbed at atmospheric pressure and high pressure$^{\delta}$ (1.0 MPa) in the different carbide-derived carbons under equilibrium conditions. CO_2/CH_4 and CO_2/N_2 selectivity derived in a kinetic regime at 25ºC and after t= 2min.